

# Bending Strength Prediction and Finite Element Analysis of Larch Structural Beams

Seung-Youp Baek, Yo-Jin Song, Hyun-Woo Kim, and Soon-Il Hong \*

The material constants of wood required for finite element analysis (FEA) are usually calculated using small clear specimens. However, defects, such as knots and slope of grain affect the strength reduction in the full-size specimens. Consequently, an error occurs if only the material constant calculated from the small clear specimens is used to predict modulus of rupture (MOR). Therefore, in this study, the MOR reduction coefficient according to defect was obtained through the bending test of the full-size specimens and applied to the FEA, in addition to the material constant from the small clear specimens. The maximum bending moment section was measured for a 3-section four-point load, and defects in the outermost tension layer were measured for laminated timber and glulam. The result of the bending test confirmed that MOR also decreased as the size of the defect increased. Therefore, when predicting MOR, a strength reduction ratio according to visual grade was applied. The MOR predicted FEA was twice as large as the actual MOR before defect correction, but the prediction error after defect correction was greatly reduced to 8%, thus increasing the prediction accuracy.

DOI: 10.15376/biores.18.1.1824-1835

Keywords: FEM; Knot; Larch; Structure beams; MOR; MOR reduction ratio

Contact information: Department of Forest Biomaterials Engineering, Kangwon National University, 1- Kangwondaehak-gil, ChunCheon-si, Gangwon-do, 24341, Republic of Korea;

\* Corresponding author: hongsi@kangwon.ac.kr

## INTRODUCTION

In general, column-beam structures are mainly used in wooden structures, which in turn use mainly timber, laminated timber, and glulam. Hand calculations were used to design the bending strength of the beam member. The transformed section method, which converts the width of the section according to the modulus of elasticity (MOE) of the layer utilized as indicated in ASTM D3737 (2003), is used primarily to forecast the modulus of rupture (MOR) of glulam (Martus 2020). Lee *et al.* (2018) used the non-destructive longitudinal vibration method and the ultrasonic measurement method to compute the non-destructive MOE of domestic larch timber. The correlation equation between the MOR after the bending test and the non-destructive MOE value was used to develop a MOR prediction formula. Song *et al.* (2018) employed the known prediction theories, the Gamma method, and the K-method, to forecast the MOR of a cross-laminated timber manufactured from larch (Song *et al.* 2018). However, both approaches pose the problem of requiring the members to be manually calculated one by one. To reduce cost and time in the area of engineering, the finite element method (FEM) has recently been applied to computer programs to actively research on strength prediction.

Structural analysis through FEM requires material density, MOE per direction, Poisson's ratio, and shear modulus, as well as the relational expression between stress and strain of the material. Because concrete is isotropic, three material constants are required: MOE in one direction, Poisson's ratio, and shear modulus. However, because wood is an orthotropic material with distinct mechanical characteristics in each direction, Finite Element Analysis (FEA) requires at least 9 material constants.

The material constant of wood may be determined in two ways: using small clear specimens or using full-size specimens. The possibility of containing defects, such as knots, increases as the size of the full-size specimen increases, resulting in lower strength values and bigger deviations (Puaad and Ahmad 2017). Consequently, it was noted that it is typically correct to obtain and utilize the material constant *via* small clear specimens for the development of a FEM that appropriately simulates the behavior of wood (Schmidt and Kaliske 2009). However, the material constant is a value determined from small clear specimens, and MOR prediction of the full-size specimens has limitations because defects, such as knots and grain slope, are not included in the small clear specimens. Gao *et al.* (2015) demonstrated that there was some error as a consequence of predicting the MOR without considering defects in the structural wooden beam by FEA. Kim (2011) performed FEM analysis after bending tests for Douglas-fir species and stated that the maximum load was predicted by FEM within the range of actual values, which were not accurate, and only demonstrated the feasibility of application. Monteiro *et al.* (2020) also verified that glulam's FEM analysis anticipated a greater MOR than the actual value.

In this study, material constants were calculated from small clear specimens of domestic larch. The MOR reduction coefficient according to the size of defects was also obtained through bending test of full-size specimens and applied to FEM analysis. Small clear specimens were prepared and the material constant was calculated to obtain the representative material constant of domestic larch required for FEA. The same MOE was used to calculate the MOR reduction ratio according to the visual grade, while domestic larch structural beams were fabricated according to the visual grade. For the visual grade, the maximum bending moment section was measured under a 3-section four-point load. For laminated timber and glulam, defects in the outermost tensile layer material were measured. After the bending test, the MOR reduction ratio was calculated according to the visual grade. In the FEM analysis, the material constant calculated from small clear specimens was applied as a representative value. Furthermore, the MOR reduction ratio according to the visual grade obtained through the bending test was applied.

## EXPERIMENTAL

### Calculation of the Representative Material Constant of Domestic Larch for FEA

The domestic larch (*Larix kaempferi* Carr.) was used in this study. Larch was purchased from the National Forestry Cooperative Federation (Yeoju-si, Korea). Structural analysis through FEM requires material density, direction MOE, Poisson's ratio, and shear MOE. To calculate the MOE and Poisson's ratio for each direction of domestic larch, a compressive strength specimen with a cross-section of 20 mm × 20 mm and a length of 60 mm was fabricated according to ISO 13061-17 (2017). A compressive strength test was subsequently performed. The Poisson's ratio was calculated using a biaxial strain gauge (FCA-5-11-1LJB, Tokyo Sokki Kenkyuio, Tokyo, Japan). A total of 20 specimens in 3

types were fabricated according to the load direction (Fig. 1). The MOE was represented by  $E_i$ , where  $i$  denotes the fiber direction (L), the tangential direction (T), and the radial direction (R) for the longitudinal direction. Poisson's ratio was expressed as  $\nu_{ij}$ , which is the strain in the  $i$ -direction with respect to the strain in the  $j$ -direction.

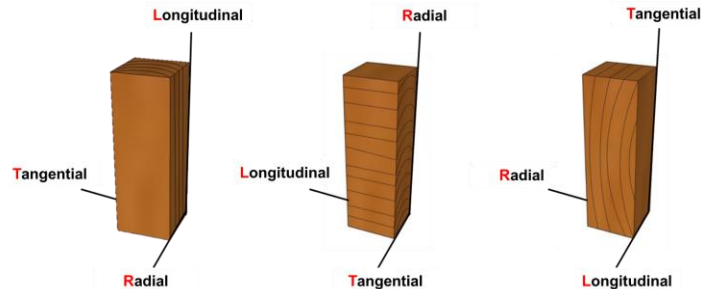


Fig. 1. Compression test specimens

The shear strength specimens were fabricated in accordance with ASTM D143 (2014) with a cross-section measuring 20 mm × 20 mm and 30 mm long, and a step difference of 10 mm × 10 mm × 10 mm. A total of 20 specimens were fabricated in three types according to the load direction (Fig. 2). The shear MOE was indicated as  $G_{ij}$ , where  $ij$  denotes the section direction (RT, TL, and LR).

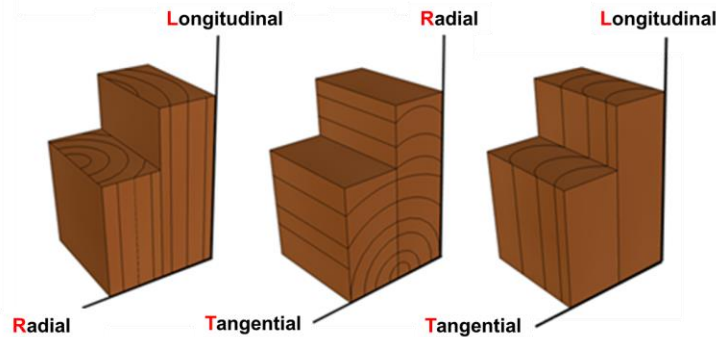


Fig. 2. Shear test specimens

## Bending Test of Domestic Larch Structural Beams for Calculation of MOR Reduction Ratio

### *Larch timber*

The domestic larch (*Larix kaempferi* Carr.) timber used in this study was 3600 mm long, 89 mm wide, and 120 mm thick. The average air-dried specific gravity was  $0.58 \pm 0.04$ , and the average air-dried moisture content was  $11.5 \pm 0.7\%$ . Larch was classified by visual grade based on defects observed on the surface of structural materials with the naked eye based on KS F 3020 (2018), softwood structural lumber, and by measuring knot diameter and slope of grain. Only the defects in the maximum bending moment section were measured under a three-section four-point load. Moreover, only defects in the tensile region were considered because defects have a greater effect on the tensile region than on the compressed region of the member (Saad and Lengyel 2022). Based on the quality standards of type 2 beams among the quality standards of visual grade structural materials, grades 1, 2, and 3 were classified according to the knots and slope of grain. Larch timbers

were classified by visual grade into T1 for grade 1, T2 for grade 2, and T3 for grade 3. The specimens consisted of 30 pieces with 10 pieces per type.

### *Laminated timbers and glulam*

Laminated timbers were made of two larch timbers (thickness 89 mm, width 120 mm, length 3600 mm). The average MOE of the timbers used was 13000 MPa. Timbers were classified by visual grade through defect measurement (KS F 3021 2018). Glulam was fabricated measuring 3000 mm in length, 90 mm in width, and 150 mm in height using layer materials (thickness 30 mm, width 90 mm, length 3000 mm). The MOEs of the layers used in the laminated timber and glulam were calculated using the longitudinal vibration method (Song and Hong 2016). The MOEs of each type of specimens were similarly used to confirm the effect of strength by defects. The outermost layer material was produced by combining materials having a MOE of E14 to E15 (14000 to 15999 MPa), the outer layer material by combining materials having an MOE of E12 to E13, and the middle layer material with materials having an MOE of E11 or less.

Phenol-resorcinol formaldehyde (PRF) resin was used for bonding when fabricating laminated larch timber and glulam. The applied amount of adhesive was 400 g/m<sup>2</sup> (one-sided application), while the applied pressure was 1.0 MPa. Laminated timbers were classified into grade 1 specimens with timber visual grade of 1 (LT1), grade 2 specimens (LT2), and grade 3 specimens (LT3). A total of 9 pieces were manufactured with 3 pieces per type. For glulam, the outermost tensile layer material was divided into grade 1 specimens (G1), grade 2 specimens (G2), and grade 3 specimens (G3) (Fig. 3). Three specimens were fabricated per type.

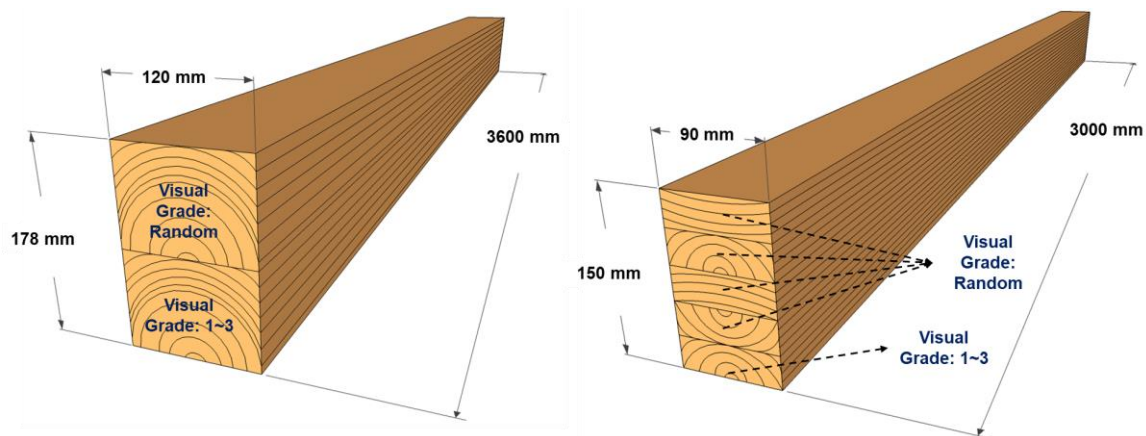


**Fig. 3.** Composition of the visual grade of laminated timber and glulam

### *Bending test*

The bending test was performed with a 3-section 4-point load (Fig. 4). The span-depth ratios of larch timber, laminated timber, and glulam were set to 15:1, 18.3:1, and 18:1, respectively, as per EN 408 (2010). The test speed was 10 mm/min. The deflection of the specimens was measured by installing a displacement gauge with a maximum capacity of 50 mm (CDP-50, Tokyo Sokki Kenkyujo, Japan) in front and behind the center of the specimens (global). The load and deformation data were transmitted using a data logger (TDS-303, Tokyo Sokki Kenkyujo, Japan).

MOE, MOR, and MOR reduction ratio (**MOR ratio<sub>vi</sub>**) were calculated according to Eqs. 1, 2, and 3,

$$MOE = \frac{\Delta Pa(3l^2 - 4a^2)}{48I3\Delta v} \quad (1)$$

$$MOR = \frac{3P_{max}(l-s)}{2bh^2} \quad (2)$$

$$MOR\ ratio_{vi} = \frac{MOR_{vi}}{MOR_{v1}} \quad (3)$$

where *MOE* is modulus of elasticity (MPa); *MOR* is modulus of rupture (MPa);  $\Delta P$  is proportional load (N); *l* is span length (mm);  $\Delta v$  is proportional deformation (mm); *a* is distance between supporting and loading pins (mm); *I* is Geometrical moment of inertia ( $mm^4$ ); *a* is distance between loading pins (mm);  $P_{max}$  is maximum load (N); *b* is specimen width; *h* is specimen thickness;  $MOR_{vi}$  is MOR according to the visual grade (*i* = 1, 2, 3); and  $MOR_{v1}$  is MOR with visual grade 1.

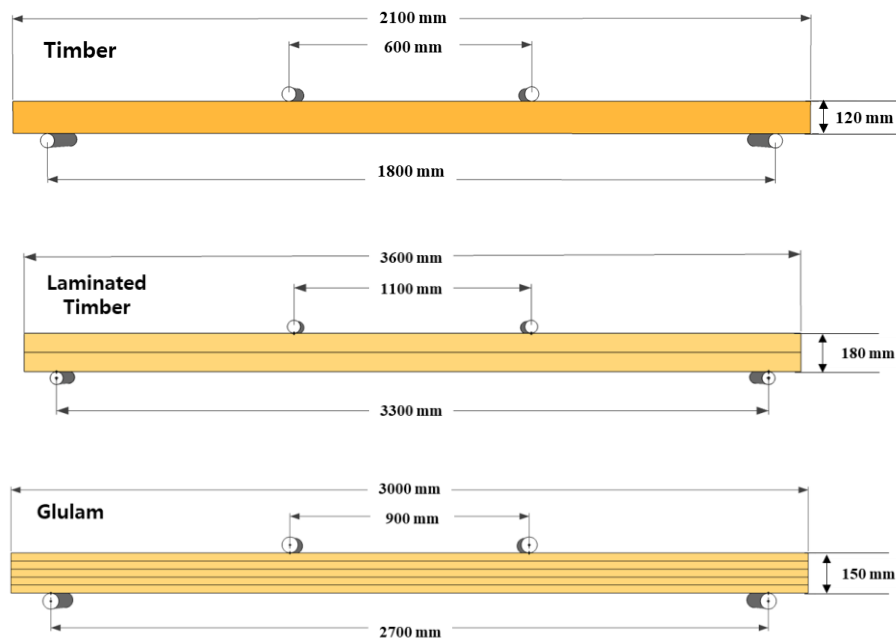


Fig. 4. Bending test set-up for timber, laminated timber, and glulam

## RESULTS AND DISCUSSION

### Material Constant of Domestic Larch

As a result of the compressive strength test, the MOE by direction was calculated as 12800 MPa ( $E_L$ ), 1170 MPa ( $E_R$ ), and 970 MPa ( $E_T$ ). The Poisson's ratio by direction was calculated as 0.357 ( $\nu_{LR}$ ), 0.493 ( $\nu_{LT}$ ), 0.026 ( $\nu_{RL}$ ), 0.606 ( $\nu_{RT}$ ), 0.412 ( $\nu_{TR}$ ), and 0.051 ( $\nu_{TL}$ ). As a result of the shear strength test result, the shear modulus by direction ( $G_{LR}$ ,  $G_{RT}$ , and  $G_{LT}$ ) was calculated as 110 MPa, 650 MPa, and 800 MPa, respectively. Thus, the data of the representative material constants of domestic larch for FEA were set up.

## Bending Test Result for Domestic Larch Structural Beams

### *Load-deflection curve and bending performance*

For small-diameter timbers with visual grades 2 and 3, the MOE ratios were 0.9 and 0.76, while the MOR ratios were 0.75 and 0.53 compared to grade 1. The MOR ratio compared to grade 1 according to the visual grade specified in the KS standard were 0.75 (grade 2) and 0.44 (grade 3), respectively. It was demonstrated that they were similar to the MOR reduction ratio according to the visual grade calculated in this study. Furthermore, it was found that defects, such as knots and slope of grain, had a greater effect on MOR than MOE. Pang *et al.* (2021) also confirmed that the knot area ratio had a greater effect on the MOR compared to the MOE.

The MOR ratio of laminated timber with visual grade 2 and 3 were 0.78 and 0.62 compared to grade 1. The MOR ratio of glulam with visual grades 2 and 3 were 0.80 and 0.68 compared to grade 1. The defects had a greater effect on the MOR of timber than laminated timber, while the MOR of glulam was relatively less affected. The MOR ratios according to the visual grade specified in the KS standard were 0.86 (grade 2) and 0.69 (grade 3), respectively. They were similar to the MOR ratios according to the visual grade calculated in this study.

It was confirmed that the MOR of the structural wood material was greatly affected by the defects in the tensile layer in the region subjected to the bending moment. This is consistent with the finding of Baek (2021) that the defect in the outermost tensile layer greatly affected the MOR of structural wood materials made of larch.

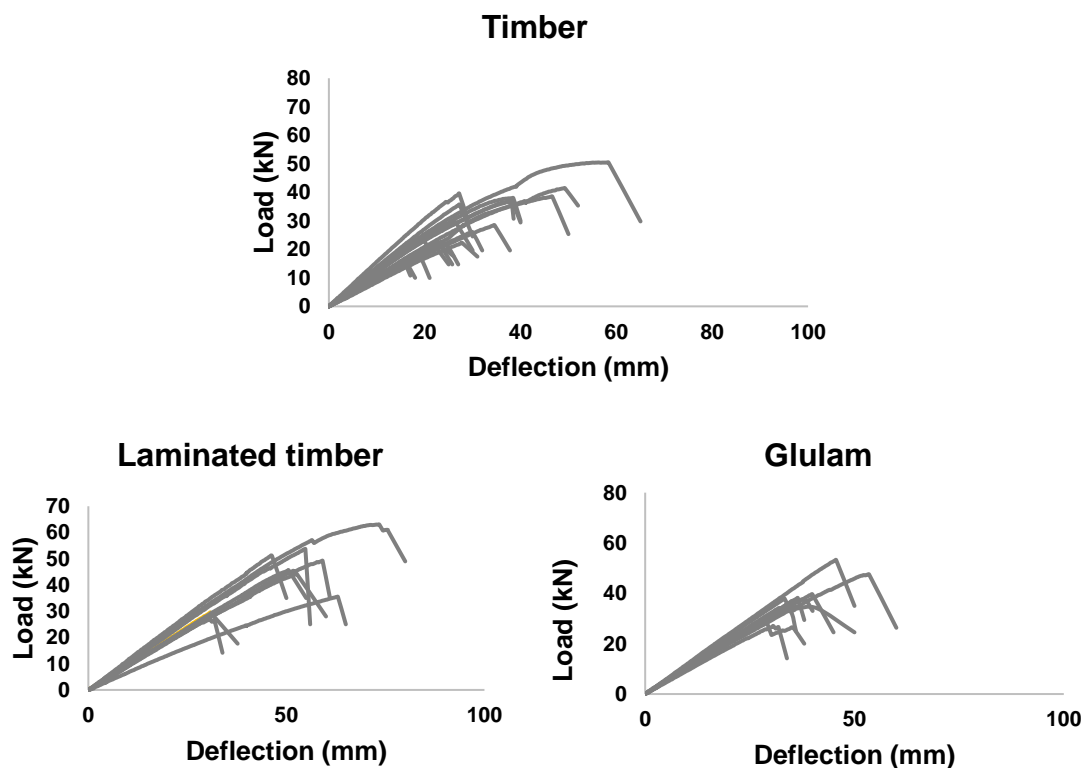


Fig. 5. Load-deflection curves of timber, laminated timber, and glulam

**Table 1.** Bending Performance of Structure Beams According to Visual Grade

		AVE. MOE (MPa)	AVE. MOR (MPa)
Timber	T1	10200	58.0
	T2	9200	41.4
	T3	7800	32.1
Laminate Timber	LT1	12700	53.2
	LT2	11000	41.8
	LT3	10400	33.2
Glulam	G1	14400	62.7
	G2	14100	50.5
	G3	13600	42.8

The FEA was performed using the data on Table 3 obtained through the bending test for the bending strength reduction ratio according to the visual grade of larch structural wood materials.

**Table 2.** MOR Reduction Ratio According to Visual Grade

Specimens	MOR Ratio <sub>v2</sub>	MOR Ratio <sub>v3</sub>
Timber	0.70	0.55
Laminated Timber	0.78	0.62
Glulam	0.80	0.68

#### *Failure mode*

As shown in Fig. 6, T1, which had no defects, was failed along the fiber slope after tensile failure at the outermost tensile region. However, T2 and T3 with defects failed at the knots as shown in Fig. 6, which caused failure at low loads and a lower MOR than T1 without defects. TPYE-LT1 without defects showed elastic behavior up to the maximum load, but at the maximum load, the failure proceeded to the compression area along the tensile area and the bonding area. It was confirmed that LT2 and LT3 with defects failed by stress concentration at the defect site. However, the elastic behavior up to the maximum load was similar for LT1, LT2, and LT3, although the failure shape of glulam varied depending on the presence or absence of defects. G1 showed elastic behavior up to the maximum load, but at the maximum load, failure started in the tensile region and continued to the compression part. Subsequently, failure occurred at the bonding surface. G2 and G3 showed elastic behavior, but after primary failure occurred at the defect site in the outermost tensile layer, the load decreased. The load increased again and the specimens finally failed at the maximum load (Fig. 5). In Glišović's study (2017), the failure mode of glulam without defects was destroyed along the fiber direction after tensile failure at the maximum bending moment between loading points, and local failure occurred at the knot when there were defects such as knots in the tensile region. Therefore, as shown in Fig. 6, Larch Structural Beams failed at a low load at the defect if there was a defect in the outermost tensile layer. Accordingly, as shown in Table 2, as the size of the defect increased, the visual grade increased, and it can be confirmed that the MOR decreased significantly.



**Fig. 6.** Failure mode of timber, laminated timber, glulam

### Prediction of Bending Strength through FEM Model

#### *Finite element analysis by FEM modeling*

Finite element analysis was performed using the ANSYS program (ANSYS 17.0). The material constants for domestic larch presented in Table 3 were used.

**Table 3.** Material Constant of Larch

Material Constant	Density (kg/m <sup>3</sup> )	$E_L$ (MPa)	$E_R$ (MPa)	$E_T$ (MPa)	$\nu_{LR}$	$\nu_{RT}$	$\nu_{LT}$	$G_{LR}$ (MPa)	$G_{RT}$ (MPa)	$G_{LT}$ (MPa)
	560	12800	1170	970	0.357	0.606	0.493	800	110	650

The support was set as fixed support. The boundary condition between the support and the specimens was set as frictional so that it could slide because it was a roller point, and the coefficient of friction was set to 0.5 (Villar-García *et al.* 2022). Because a bending test causes large deflection values, the large deflection option is set to on. The bonding condition between the layers was set to bonded. The initial substep was defined as 100, while the maximum substep was defined as 5000. The shapes of the meshes are uniformly regular hexagons. The size of the divided mesh was set to 20 mm. The number of divided elements and nodes was set to 1684 and 9874 for timber, 3368 and 19749 for laminated timber, and 8640 and 53325 for glulam, respectively (Fig. 7).

The bending strength was predicted using bilinear isotropic hardening, and the yield stress and tangent modulus were applied. For the tangent modulus, a value multiplied by 0.01 of the MOE was applied (Hong *et al.* 2014), while a yield stress of 58 MPa was used (Lee 2018). Furthermore, the MOR ratio (Table 2) according to the visual grade obtained through the bending test of the domestic larch structural member was applied to the yield stress. A strain of 50 mm in the loading direction was applied to the loading point to predict strength.

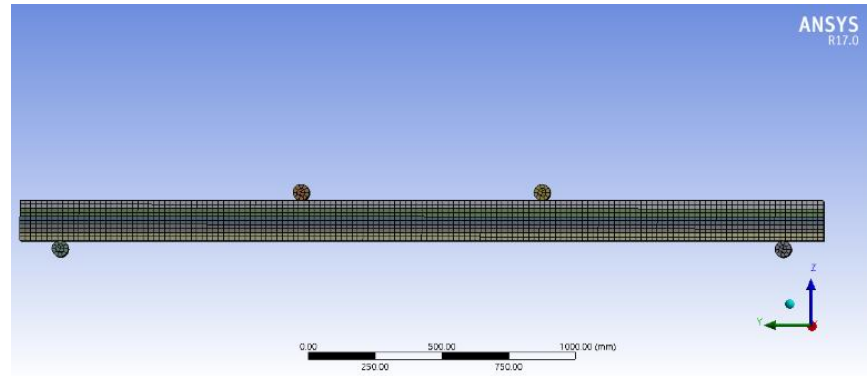


Fig. 7. Finite element analysis model of glulam

### *Predicting bending strength according to visual grade*

The bending strengths predicted through FEA ( $MOR_{FEM1}$ ) of larch timber, laminated timber, and glulam before strength correction were 62.2, 56.9, and 62.3 MPa, respectively. The errors in the predicted bending strength compared to the actual values of structural wood materials with visual grade 2 were 33%, 36%, and 23%, respectively. The bending strength prediction errors of structural wood materials with visual grade 3 were 104%, 71%, and 45%, respectively.

Subsequently, the bending strength to which the bending strength reduction ratio ( $MOR_{FEM2}$ ) was applied was predicted. After applying the bending strength reduction ratios in Table 5, the prediction errors obtained were 8%, 0%, and 6%, respectively, for structural wood materials with visual grade 2. Furthermore, the bending strength prediction errors of structural wood materials with visual grade 3 were significantly reduced to 8%, 8%, and 3%, respectively. Predicting the bending strength through FEM of conventional wood materials for structural purposes tends to cause errors because defects present in full-size specimens are not considered. Therefore, it was necessary to estimate the bending strength by considering defects such as knots and slope of grain when predicting the bending strength of structural wood materials.

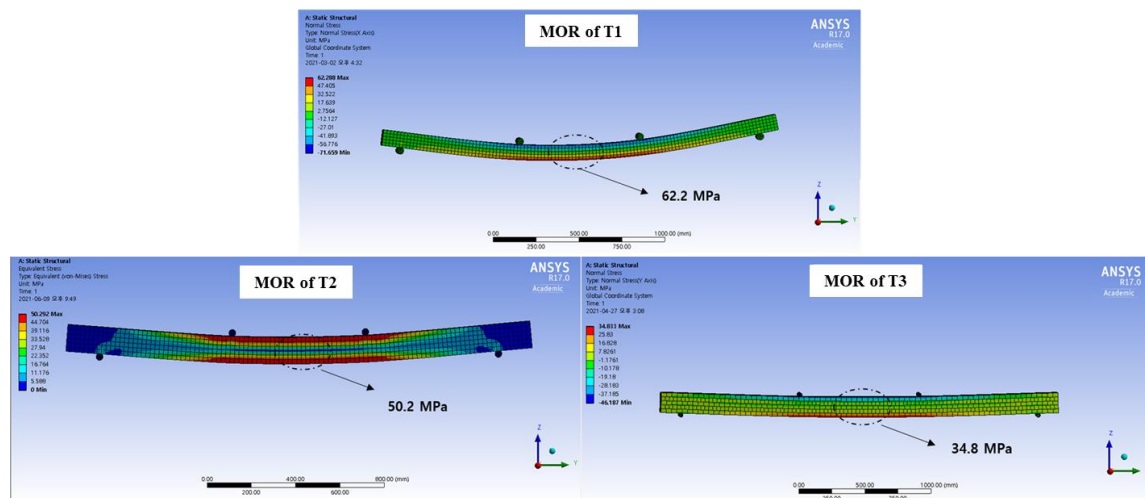


Fig. 8. MOR prediction result of SOLID WOOD by FEM model

**Table 4.** MOR Prediction Results by FEM

		MOR <sub>test</sub> (MPa)	MOR <sub>fem1</sub> (MPa)	MOR <sub>fem2</sub> (MPa)
Timber	T1	58.0 (1)	62.2 (1.07)	62.2 (1.07)
	T2	41.4 (1)	62.2 (1.33)	45.8 (0.98)
	T3	32.1 (1)	62.2 (2.04)	34.8 (1.08)
Laminated Timber	LT1	53.1 (1)	56.9 (1.07)	56.9 (1.07)
	LT2	41.8 (1)	56.9 (1.36)	42.4 (1.00)
	LT3	33.1 (1)	56.9 (1.71)	35.8 (1.08)
Glulam	G1	62.6 (1)	62.3 (1.0)	62.3 (1.0)
	G2	50.5 (1)	62.3 (1.23)	53.9 (1.06)
	G3	42.8 (1)	62.3 (1.45)	41.7 (0.97)

(): /MOR<sub>test</sub>, MOR<sub>test</sub>: MOR obtained by bending test, MOR<sub>fem1</sub>: MOR of FEM before intensity correction, MOR<sub>fem2</sub>: MOR of FEM after intensity correction

## CONCLUSIONS

Finite element analysis (FEA) in the wood structure field is applied by calculating the material constant using small clear specimens. However, defects, such as knots and slope of grain, exist in the full-size specimens, and these defects greatly affect the reduction in maximum load that can be endured by full-size specimens. Bending strength prediction through FEA of beam members, such as timber, laminated timber, and glulam, was performed by applying the bending strength reduction ratio according to the size of the defect using a bending test as well as the material constant obtained from the small clear specimens.

1. The material constant of domestic larch required for FEA was constructed using small clear specimens. The constructed data was used as a representative value of domestic larch, while the bending strength of a full-size specimens was predicted by applying a bending strength reduction ratio according to the visual grade obtained through the bending test.
2. The result was subsequently compared with the measured value. Before the strength reduction ratio correction, specimens with defects generated a large difference between the predicted and measured bending strength values. However, after applying the bending strength reduction ratio, the predicted value was predicted similar to the measured bending strength value even if there was a defect. This suggests that defects must be considered to accurately predict the bending strength of structural wooden beams.

## ACKNOWLEDGEMENTS

This study was conducted as a basic research project supported by the Korea Research Foundation with funding from the Korean Ministry of Education in 2016 (Grant No. R1D1A1B01011163).

## REFERENCES CITED

- ASTM D143 (2014). “Standard test methods for small clear specimens of timber,” ASTM International, West Conshohocken, PA, USA.
- ASTM D3737-03 (2019). “Standard practice for establishing allowable properties for structural glued laminated timber (glulam),” ASTM International, West Conshohocken, PA, USA.
- Baek, S. Y., Song, Y. J., Yu, S. H., Kim, D. H., and Hong, S. I. (2021). “Bending performance of cross-laminated timber-concrete composite slabs according to the composite method,” *BioResources* 16(4), 8227-8238. DOI: 10.15376/biores.16.4.8227-8238
- EN 408 (2010). “Timber structures – Structural timber and glued laminated timber – Determination of some physical and mechanical properties,” European Committee for Standardization, Brussels, Belgium.
- Gao, Y., Wu, Y., Zhu, X., Zhu, L., Yu, Z., and Wu, Y. (2015). “Numerical analysis of the bending properties of cathay poplar glula,” *Materials* 8(10), 7059-7073. DOI: 10.3390/ma8105362
- Glišović, I., Pavlović, M., Stevanović, B., and Todorović, M. (2017). “Numerical analysis of glulam beams reinforced with CFRP plates,” *Journal of Civil Engineering and Management* 23(7), 868-879. DOI: <https://doi.org/10.3846/13923730.2017.1341953>
- Hong, J. P., Kim, C. K., Lee, J. J., and Oh, J. K. (2014). “Elasto-plastic anisotropic wood material model for finite solid element applications,” *Journal of the Korean Wood Science and Technology* 42(4), 367-375. DOI: 10.5658/wood.2014.42.4.367
- ISO 13061-17 (2017). “Physical and mechanical properties of wood—test methods for small clear wood specimens—Part 17: Determination of ultimate stress in compression parallel to grain,” International Organization for Standardization, Geneva, Switzerland.
- Kim, G.-C. (2011). “A study on the bending performance of structural size lumbers using the ANSYS,” *Journal of the Korea Furniture Society* 22(4), 323-329.
- Lee, I.-H., Cho, S.-M., and Hong, S.-I. (2018). “Prediction of the MOR of larch lumber,” *Journal of the Korean Wood Science and Technology* 46(1), 93-99. DOI: 10.5658/wood.2018.46.1.93
- KS F 3020 (2018). “Softwood structural lumber,” Korean Standards Association, Seoul, Korea.
- KS F 3021 (2018). “Structural glued laminated timber,” Korean Standards Association, Seoul, Korea.
- Martus, M. (2020). *Calculation Tool for Estimation of the Material Properties of Glulam Beams with Known Layout*, Master’s Thesis, Aalto University, Espoo, Finland.
- Monteiro, S. R., Martins, C., Dias, A. M., and Cruz, H. (2020). “Mechanical performance of glulam products made with Portuguese poplar,” *European Journal of Wood and Wood Products* 78(5), 1007-1015. DOI: 10.1007/s00107-020-01569-y

- Pang, S. J., Shim, K. B., and Kim, K. H. (2021). "Effects of knot area ratio on the bending properties of cross-laminated timber made from Korean pine," *Wood Science and Technology* 55(2), 489-503. DOI: 10.1007/s00226-020-01255-5
- Puaad, M. B. F. M., and Ahmad, Z. (2017). "Comparing the compressive strength properties of structural size and small clear specimens for Malaysian tropical timber," *Science International* 29(1), 25-25. DOI: 10.1063/1.5062660
- Saad, K., and Lengyel, A. (2022). "Accurate finite element modelling of knots and related fibre deviations in structural timber," *Journal of King Saud University-Engineering Sciences* (In Press). DOI: 10.1016/j.jksues.2022.01.005
- Schmidt, J., and Kaliske, M. (2009). "Models for numerical failure analysis of wooden structures," *Engineering Structures* 31(2), 571-579. DOI: 10.1016/j.engstruct.2008.11.001
- Song, Y. J., and Hong, S. I. (2016). "Evaluation of bonding strength of larch cross-laminated timber," *Journal of the Korean Wood Science and Technology* 44(4), 607-615. DOI: 10.5658/WOOD.2016.44.4.607
- Song, Y. J., and Hong, S. I. (2018). "Performance evaluation of the bending strength of larch cross-laminated timber," *Wood Research* 63(1), 105-116.
- Villar-García, J. R., Vidal-López, P., Rodríguez-Robles, D., and Moya Ignacio, M. (2022). "Friction coefficients of chestnut (*Castanea sativa* Mill.) sawn timber for numerical simulation of timber joints," *Forests* 13(7), 1078-1094. DOI: <https://doi.org/10.3390/f13071078>

Article submitted: November 14, 2022; Peer review completed: December 31, 2022;  
Revised version received and accepted: January 2, 2023; Published: January 19, 2023.  
DOI: 10.15376/biores.18.1.1824-1835